

## Hydrogen Bonds in GlcNAc( $\beta$ 1,3)Gal( $\beta$ )OME in DMSO Studied by NMR Spectroscopy and Molecular Dynamics Simulations

Gyuchang Shim, Jaemin Shin,<sup>†</sup> and Yangmee Kim\*

*Department of Chemistry, Konkuk University, Seoul 143-701, Korea*  
<sup>†</sup>*IDRTech Inc., 461-6 Jeonmin-dong, Yusung-gu, Daejeon 305-390, Korea*  
*Received October 29, 2003*

Hydrogen bond is an important factor in the structures of carbohydrates. Because of great strength, short range, and strong angular dependence, hydrogen bonding is an important factor stabilizing the structure of carbohydrate. In this study, conformational properties and the hydrogen bonds in GlcNAc( $\beta$ 1,3)Gal( $\beta$ )OME in DMSO are investigated through NMR spectroscopy and molecular dynamics simulation. Lowest energy structure in the adiabatic energy map was utilized as an initial structure for the molecular dynamics simulations in DMSO. NOEs, temperature coefficients, SIMPLE NMR data, and molecular dynamics simulations proved that there is a strong intramolecular hydrogen bond between O7' and HO3' in GlcNAc( $\beta$ 1,3)Gal( $\beta$ )OME in DMSO. In aqueous solution, water molecule makes intermolecular hydrogen bonds with the disaccharides and there was no intramolecular hydrogen bonds in water. Since DMSO molecule is too big to be inserted deep into GlcNAc( $\beta$ 1,3)Gal( $\beta$ )OME, DMSO can not make strong intermolecular hydrogen bonding with carbohydrate and increases the ability of O7' in GlcNAc( $\beta$ 1,3)Gal( $\beta$ )OME to participate in intramolecular hydrogen bonding. Molecular dynamics simulation in conjunction with NMR experiments proves to be efficient way to investigate the intramolecular hydrogen bonding existed in carbohydrate.

**Key Words :** GlcNAc( $\beta$ 1,3)Gal( $\beta$ )OME, NMR spectroscopy, SIMPLE NMR, Molecular dynamics simulation, Hydrogen bond

### Introduction

NMR is a good method to obtain structural data of carbohydrate in solution where motional variations are less restricted than in crystals. Also, in many cases, the crystal structures of carbohydrates are not available. However, because of severe spectral overlaps, NMR experiments do not provide enough NOE distance constraints to allow a complete structure determination of carbohydrates.<sup>1-5</sup> Sometimes, theoretical modeling of carbohydrates can provide more informations.<sup>6-15</sup>

Hydrogen bonding is an important factor stabilizing the structure of carbohydrate. Carbohydrates have hydroxyl groups that can simultaneously donate and accept protons of hydrogen bonds.<sup>14,15</sup> NMR techniques such as chemical shift variation, temperature coefficients, nuclear Overhauser effects, and coupling constant have been used to investigate the hydrogen bonds in carbohydrate structures.<sup>3,16-20</sup>

Here, we studied the hydrogen bond existed in the structure of GlcNAc( $\beta$ 1,3)Gal( $\beta$ )OME in DMSO. Repeating units of this disaccharide are present in certain mucins, membrane glycoproteins, and polyglycosylceramides where they are associated with the i-antigenic structures and serve as precursors of the ABH, Lewis, and P1 blood group antigens.<sup>21,22</sup> Previously, we reported the two probable structures of GlcNAc( $\beta$ 1,3)Gal( $\beta$ )OME in water which are in dynamic equilibrium. No intramolecular hydrogen bonds

has been found for GlcNAc( $\beta$ 1,3)Gal( $\beta$ )OME in water.<sup>2</sup> Since DMSO molecule is too big to be inserted deep into GlcNAc( $\beta$ 1,3)Gal( $\beta$ )OME, DMSO can not make strong intermolecular hydrogen bonding with carbohydrate and increases the ability of hydroxyl groups in carbohydrates to participate in intramolecular hydrogen bonding. In this study, we have utilized molecular dynamics simulations in DMSO box in conjunction with NMR spectroscopy to examine intramolecular hydrogen bonding in GlcNAc( $\beta$ 1,3)-Gal( $\beta$ )OME in DMSO.

### Experimental Section

**Nomenclature.** Figure 1 shows the naming scheme of the GlcNAc( $\beta$ 1,3)Gal( $\beta$ )OME molecule. Flexibilities around the glycosidic linkages are described by torsion angles:  $\Phi$  and  $\Psi$  defined by H1'-C1'-O3-C3 and C1'-O3-C3-H3, respectively.  $\chi$  is O5-C5-C6-O6. Three possible orientations relative to C5 and C6 are designated as GT, GG, and TG as described in the previous paper.<sup>2</sup>  $\theta$ , C1'-C2'-N2'-C7' determines the orientation of N-acetyl group.

**NMR Experiments.** GlcNAc( $\beta$ 1,3)Gal( $\beta$ )OME was purchased from Sigma. The NMR samples for the resonance assignment were dissolved in 100% DMSO- $d_6$  under nitrogen gas and 10 mM sample was made in 0.45 mL. NMR experiments were performed at 25 °C on a Bruker AMX 500 MHz spectrometer at Korea Basic Science Institute. All the data were processed off-line using FELIX software on SGI workstation in Department of Chemistry at Konkuk University.<sup>23</sup> For spectral assignments a double

\*To whom correspondence should be addressed. Phone: +82-2-450-3421; Fax: +82-2-447-5987; e-mail: ymkim@konkuk.ac.kr

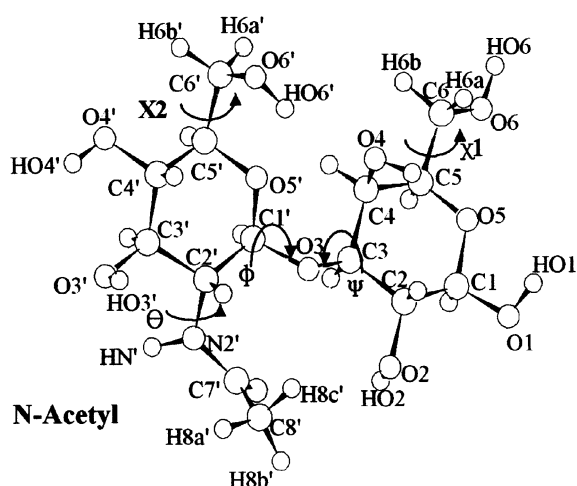


**Figure 1.** Schematic structure of GlcNAc( $\beta$ 1,3)Gal( $\beta$ )OMe. The dihedral angles,  $\Phi$ ,  $\Psi$ ,  $\chi_1$ ,  $\chi_2$ , and  $\theta$  are defined as H1'-C1'-O3-C3, C1'-O3-C3-H3, O5'-C5'-C6'-O6, O5'-C5'-C6'-O6', and C1'-C2'-N2'-C7', respectively.

quantum filtered COSY spectrum was obtained using time proportional phase incrementation (TPPI) with spectral width of 1754.386 Hz, 2048  $t_2$  point, and 512  $t_1$  point.<sup>24</sup> We collected a TOCSY spectrum with a mixing time of 80 msec and a  $^1\text{H}$ - $^{13}\text{C}$  heteronuclear multiple quantum coherence (HMQC) spectrum to aid the spectral assignments.<sup>25-27</sup> 2D  $^1\text{H}$ - $^1\text{H}$  phase sensitive NOESY and ROESY experiment was performed with mixing times of 600 and 800 msec.<sup>28,29</sup> In order to calculate temperature coefficients, chemical shifts were measured every  $5^\circ$  from 298 K to 333 K.

Sample for the measurement of the deuterium isotope effect on chemical shifts was deuterated and dried by lyophilizing from  $\text{D}_2\text{O}$ /acetone solutions and then dissolved in dry DMSO- $d_6$ . NMR sample was made by mixing adequate amounts of protiated and deuterated GlcNAc-( $\beta$ 1,3)Gal( $\beta$ )OMe. The signs and the magnitudes of the chemical shift variation from the isotope effects was determined by SIMPLE (Secondary Isotope Multiplets NMR spectroscopy of Partially Labeled Entities)  $^1\text{H}$  NMR measurement.<sup>16,18</sup>

**Molecular dynamics simulations of GlcNAc( $\beta$ 1,3)-Gal( $\beta$ )OMe.** In order to investigate the dynamic behavior of the GlcNAc( $\beta$ 1,3)Gal( $\beta$ )OMe, molecular dynamics simulations on GlcNAc( $\beta$ 1,3)Gal( $\beta$ )OMe in DMSO was proceeded. All calculations were performed with CHARMM (Chemistry at HARvard Macromolecular Mechanics). The potential function of CHARMM is as follows<sup>30</sup>;

$$V(q) = \sum k_{bi}(r_i - r_{0i})^2 + \sum k_{\theta i}(\theta_i - \theta_{0i})^2 + \sum k_{UBi}(s_i - s_{0i})^2 + \sum k'_{UBi}(s_i - s_{0i})^2 + \sum k_{\phi i}[1 + \cos(n_i\phi_i - \delta_i)] + \sum k_{\omega i}(\omega_i - \omega_{0i})^2 + \sum \left( \frac{A_{ij}}{r_{ij}^{12}} - \frac{B_{ij}}{r_{ij}^6} \right) + \sum \frac{a_i a_j}{4\pi\epsilon_0 r_{ij}}$$

This equation contains the terms such as bond energy, angle energy, dihedral energy, Urey-Bradley 1-3 interaction energy, improper energy, electrostatic energy, and van der

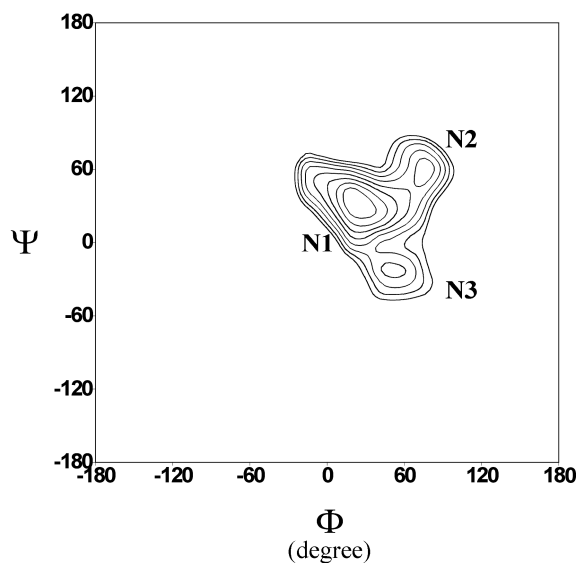


**Figure 2.** 5 Adiabatic energy map of GlcNAc( $\beta$ 1,3)Gal( $\beta$ )OMe generated in vacuum<sup>2</sup>. Contours are in 0.5 kcal/mol intervals from 0.5 to 5.0 kcal/mol above the energy minimum. Three low energy structures are designated as N1, N2 and N3.

Waals energy. Hydrogen bond energy term is not handled separately, but treated as nonbonding interactions in the CHARMM potential. Parameters used here are available through QUANTA.<sup>23</sup>

The conformational behavior of GlcNAc( $\beta$ 1,3)Gal( $\beta$ )OMe was examined through the dynamics simulation with explicit DMSO molecules. For the simulations a cubic DMSO box (density 1.1) consisting of 125 DMSO molecules with a length of 24.52 Å in each dimension was set-up. Parameters for DMSO molecules were adopted from reference.<sup>31</sup> They were equilibrated for 40 ps and 300 ps molecular dynamics simulations were performed before carbohydrate molecule was positioned in the center of the DMSO box.<sup>32-34</sup> In the previous paper, adiabatic energy map of GlcNAc( $\beta$ 1,3)-Gal( $\beta$ )OMe in vacuum was calculated and it has three low energy minima as shown in Figure 2.<sup>2</sup> Since the lowest energy structure N1 in adiabatic energy map satisfies well the NMR data of GlcNAc( $\beta$ 1,3)Gal( $\beta$ )OMe in DMSO, it was utilized in generating initial geometries of GlcNAc-( $\beta$ 1,3)Gal( $\beta$ )OMe. All solvent molecules closer than 2.8 Å to any heavy atom of the carbohydrate molecule were deleted.<sup>1</sup> 5000 cycles of ABNR energy minimization were carried out, keeping the carbohydrate harmonically constrained to its original structure. During the whole simulations, minimum-image periodic boundary conditions were used to eliminate edge effects. The simulation involved an equilibration period of 40 ps and the production run was performed for 300 ps, from which the dynamics trajectory was obtained for the conformational analysis. Simulations and analysis were performed on a SGI O2 workstation and Cray-C90 supercomputer at SERI.

## Results and Discussion

### Resonance Assignment and NOE Measurement. The

**Table 1.**  $^1\text{H}$  and  $^{13}\text{C}$  chemical shifts of GlcNAc( $\beta$ 1,3)Gal( $\beta$ ) in DMSO- $d_6$ 

Proton	$\delta$ (ppm) <sup>a</sup>	Carbon	$\delta$ (ppm) <sup>b</sup>
H1'	4.60	C1'	102.01
H2'	3.35	C2'	55.69
H3'	3.33	C3'	70.41
H4'	3.10	C4'	69.36
H5'	3.10	C5'	76.68
H6a'	3.65	C6'	60.31
H6b'	3.46	C7'	170.14
HN'	7.62		
HO3'	5.00 (-5.1) <sup>b</sup>		
HO4'	4.97 (-6.6) <sup>b</sup>		
HO6'	4.44 (-7.3) <sup>b</sup>		
<hr/>			
H1	4.05	C1	103.92
H2	3.40	C2	56.48
H3	3.36	C3	82.32
H4	3.84	C4	67.13
H5	3.40	C5	74.80
H6a	3.53	C6	60.87
H6b	3.98		
HO2	4.66 (-8.6) <sup>b</sup>		
HO4	4.04 (-8.0) <sup>b</sup>		
HO6	4.55 (-7.6) <sup>b</sup>		
OMe	3.38		

<sup>a</sup>Chemical shift of TMS peak was set at 0 ppm. <sup>b</sup>Temperature coefficients (ppb/K) of hydroxyl groups in GlcNAc( $\beta$ 1,3)Gal( $\beta$ ) in DMSO- $d_6$ .

proton resonance assignment in GlcNAc( $\beta$ 1,3)Gal( $\beta$ )OMe in DMSO was proceeded on the basis of DQF-COSY, NOESY, and HMQC spectra. Heteronuclear correlated experiments such as HMQC and HMBC were used to complete assignment. Table 1 lists  $^1\text{H}$  and  $^{13}\text{C}$  chemical shifts. Chemical shifts of most of the ring protons are crowded between 3.0 and 3.7 ppm except the anomeric protons. Amide proton in the N-acetyl group and all the hydroxyl protons are exchanged with deuterium within 5 minutes.

Table 1 also shows the temperature coefficients of the amide and hydroxyl protons. A reduction in temperature susceptibility (ppb/deg) has been commonly accepted as an indicator of reduced interaction with solvent, due to intramolecular hydrogen bonding. A relatively smaller temperature coefficient is observed for HO3' proton than for the other hydroxyl protons. This may correspond to a transfer of electron density from the OH bond as a result of hydrogen bonding with the other atoms as electron donors.

Distance informations derived from NOE data should lead to definition of the solution structure. The distance informations obtained from NOESY and ROESY experiments with mixing times of 600 msec and 800 msec are listed in Table 2. Particular interest should be imposed on the protons around the glycosidic linkage. The interresidue NOEs such as H1'-H2, H1'-H3, and H1'-H4 are very important to determine the conformation of disaccharide. For the calibration, distance between H1-H2 was set to 3.1 Å and this distance is the value in charmm-minimized structures.

**Table 2.** Conformational features of GlcNAc( $\beta$ 1,3)Gal( $\beta$ ) obtained from averaged dynamics trajectories generated in DMSO box

	Initial structure N1 <sup>2</sup>	Average values in MD simulation	NMR data (Å)
$\Phi^b$	20 <sup>a</sup>	61.7 ( $\pm$ 9.9) <sup>a</sup>	
$\Psi^b$	40	30.2 ( $\pm$ 10.0)	
$\chi^b$	19	0.5 ( $\pm$ 12.3)	
$\chi^b$	35	5.7 ( $\pm$ 17.8)	
$\theta^b$	155	152.2 ( $\pm$ 7.7)	
H1'-H2 <sup>c</sup>	3.5 <sup>c</sup>	3.4 ( $\pm$ 0.2) <sup>c</sup>	3.8
H1'-H3 <sup>c</sup>	2.4	2.8 ( $\pm$ 0.2)	3.0
H1'-H4 <sup>c</sup>	4.3	4.5 ( $\pm$ 0.1)	4.3
HO2-HN <sup>c</sup>	4.0	4.4 ( $\pm$ 0.4)	4.4
O7'--HO3'-O3'	2.1	2.1 ( $\pm$ 0.5) <sup>c</sup>	
		142.5 ( $\pm$ 29.8) <sup>b</sup>	
		0.74 <sup>d</sup> (1.9 <sup>e</sup> , 156.8 <sup>f</sup> )	

<sup>a</sup>Numbers in the parenthesis are the rms deviations from the averaged values. <sup>b</sup>Angles are in degree. <sup>c</sup>Distances are in Å. <sup>d</sup>Occurrence probability that bond distance is less than or equal to 2.5 Å and angle is greater than or equal to 135°. <sup>e</sup>Average distance during bond distance is less than or equal to 2.5 Å. <sup>f</sup>Average angle during angle is greater than or equal to 135°.

**Simple NMR.** For molecules with partially deuterated hydroxyl groups observed under conditions of slow exchange, intramolecular hydrogen bonding between hydroxyl groups is manifested by isotopically shifted hydroxyl proton resonances. This phenomenon has been termed SIMPLE NMR because it entails the observation of Secondary Isotope Multiplets of Partially Labeled Entities (SIMPLE). According to the previous work on sucrose, it was found that the hydroxyl group acting as donor exhibits a negative (to low frequency) isotope shift, when the hydrogen atom in hydroxyl group as an acceptor is replaced by deuterium.<sup>18</sup>  $^1\text{H}$  NMR spectrum of the hydroxyl proton resonances of GlcNAc( $\beta$ 1,3)Gal( $\beta$ )OMe in DMSO- $d_6$  is shown in Figure 3. OH3' shows the doublets due to the vicinal coupling to the methine protons. The SIMPLE  $^1\text{H}$  NMR spectrum (OH : OD = 1 : 1) in DMSO- $d_6$  exhibits resolved isotopically shifted resonance signals for OH3'. The OH3' resonance exhibits negative isotope effect ( $-3.52 \times 10^{-3}$  ppm). Isotope effect observed for OH3' resonances is transmitted through an intramolecular hydrogen bond between OH3' and some other hydrogen bond acceptor. This isotope effect observed for OH3' is caused by deuterium substitution of hydroxyl group able to form hydrogen bonds to the other. There were no isotope effects found for the other hydroxyl protons. NMR data can prove that there is an intramolecular hydrogen bond between OH3' and acceptor, but it is not enough to determine the exact location and the stability of hydrogen bond.

NMR experiments of carbohydrate in water are usually performed in D<sub>2</sub>O and all the hydroxyl protons which can give the useful informations about hydrogen bondings in carbohydrates are exchanged with deuterium. Since hydroxyl protons in sugar rings can not be exchanged with deuterium in DMSO- $d_6$ , NMR experiments of carbohydrates in DMSO give useful information about hydrogen bonds in

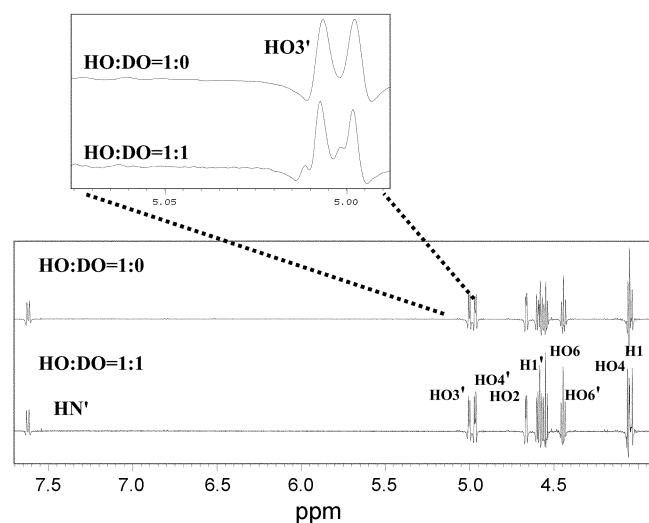


**Figure 3.** 500 MHz  $^1\text{H}$  NMR spectrum of the hydroxyl protons resonances of GlcNAc( $\beta$ 1,3)Gal( $\beta$ ) in DMSO- $d_6$  at OH:OD ratios of 1 : 0 and 1 : 1. In the upper box, expanded  $^1\text{H}$  NMR spectrum of the OH3' hydroxyl proton resonance in DMSO- $d_6$ .

carbohydrates as shown in this result.

**Molecular Dynamics Simulations in DMSO Box.** In order to investigate the hydrogen bond existed in DMSO, molecular dynamics simulations with explicit DMSO molecules were performed. Table 2 shows the conformational features of GlcNAc( $\beta$ 1,3)Gal( $\beta$ )OMe obtained from the average dynamical trajectory generated in DMSO box. As listed in Table 2, MD trajectory in DMSO box fluctuates near the N1 conformation but it does not located exactly on the N1 state. The averaged value of  $\Phi$  dihedral angle was  $61.7^\circ$  and that of  $\Psi$  was  $30.2^\circ$ . The orientation of exocyclic hydroxymethyl groups of both rings and the orientation of N-acetyl group are retained. All the average distances agree well with the NOE data. As listed in Table 2 the intramolecular hydrogen bond, O7'-OH3' was maintained through the trajectory. Averaged O7'-OH3' distance was 2.1 Å. The intramolecular hydrogen bond O7'-OH3' in the final shot of MD simulation of GlcNAc( $\beta$ 1,3)Gal( $\beta$ ) is shown in Figure 4. In order to understand the details about the hydrogen bonds observed during the simulation, we looked

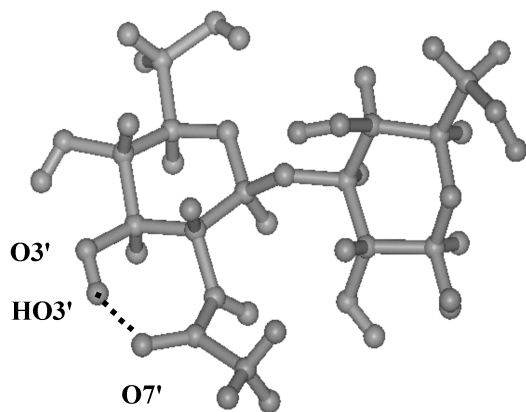


**Figure 4.** The intramolecular hydrogen bond O7'-OH3' in the final shot of MD simulation of GlcNAc( $\beta$ 1,3)Gal( $\beta$ ).

at the occurrence of the hydrogen bonds as listed in Table 2. We calculated the occurrence of the hydrogen bond by counting how frequently the distance between the hydrogen atom and the acceptor was  $r_{\text{ha}} < 2.5 \text{ \AA}$  and the angle between the donor, the hydrogen atom and the acceptor is greater than  $135^\circ$ , simultaneously. Hydrogen bond between O7'-HO3'-O3' is frequently observed with an occurrence of 0.74 and is also strong as measured by the distance of 1.9 Å and the angle of  $156.8^\circ$ .

## Conclusion

Hydrogen bond is an important factor in the structures of carbohydrates. Because of great strength, short range, and strong angular dependence, hydrogen bonding is an important factor stabilizing the structure of carbohydrate. Structures of carbohydrates such as gangliosides and many different kinds of disaccharides or trisaccharides have been determined in water or DMSO by NMR spectroscopy.<sup>1-5,16-20</sup> Water molecule is well known to make strong hydrogen bond with carbohydrate in the aqueous solution because it is very polar and small enough to be inserted deep into the disaccharide and weaken the intramolecular hydrogen bonds in carbohydrates. DMSO is much bigger than water and it is not easy to be inserted deep into the disaccharide. As reported in the previous paper, GlcNAc( $\beta$ 1,3)Gal( $\beta$ )OMe in water does not have any intramolecular hydrogen bonds and it exists in two conformationally discrete forms between N2 and N3 conformations in water.<sup>2</sup> MD trajectory in DMSO fluctuates near N1 state in the adiabatic energy map and satisfies the experimental NMR data well. N1 trajectory is not located exactly at the N1 state but this might be happened because energy map calculation in vacuum can not represent the solvent effect of DMSO perfectly. However, since it is impossible to carry out an energy map calculation of carbohydrate in the solvent environment with explicit DMSO molecules, molecular dynamics simulation in conjunction with NMR experiments proves to be efficient ways to investigate the intramolecular hydrogen bonding existed in carbohydrate in DMSO. Although NMR methods are used to indicate the presence of hydrogen bondings in carbohydrates, they are usually unable to discriminate between the donor and acceptor hydroxyl groups or to provide a basis for comparison of the relative strengths of hydrogen bonds in these molecules. Molecular dynamics simulations in explicit DMSO molecules can provide these informations. By using the data obtained from the NOEs, temperature coefficients, SIMPLE NMR data, and molecular dynamics simulations, we can conclude that there are stable intramolecular hydrogen bond between O7' and HO3' in GlcNAc( $\beta$ 1,3)Gal( $\beta$ )OMe. Molecular dynamics simulation in conjunction with NMR experiments proves to be efficient way to investigate the intramolecular hydrogen bonding existed in carbohydrate.

**Acknowledgments.** This work was supported by Konkuk University in 2002.

## References

1. Cheong, Y.; Shim, G.; Kang, D.; Kim, Y. *J. Mol. Struct.* **1999**, 475, 219.
  2. Shim, G.; Lee, S.; Kim, Y. *Bull. Korean Chem. Soc.* **1997**, 18, 415.
  3. Lee, K.; Lee, S.; Jhon, G.; Kim, Y. *Bull. Korean Chem. Soc.* **1998**, 19, 566.
  4. Kozar, T.; Tvaroska, I.; Carver, J. P. *Glycoconj. J.* **1998**, 15(2), 187.
  5. Hoog, C.; Rotondo, A.; Johnston, B. D.; Pinto, B. M. *Carbohydr. Res.* **2002**, 337, 2023.
  6. Oh, J.; Kim, Y.; Won, Y. *Bull. Korean Chem. Soc.* **1995**, 16, 1153.
  7. Tvaroska, I.; Taravel, F. R.; Utille, J. P.; Carver, J. P. *Carbohydr. Res.* **2002**, 337, 353.
  8. Kuttel, M.; Brady, J. W.; Naidoo, K. J. *J. Comput. Chem.* **2002**, 3, 1236.
  9. Naidoo, K. J.; Denysyk, D.; Brady, J. W. *Protein Eng.* **1997**, 10, 1249.
  10. Brady, J. W.; Schmidt, R. K. *J. Phys. Chem.* **1993**, 97, 958.
  11. Stevansson, B.; Høeog, C.; Ulfstedt-Jaekel, K.; Huang, Z.; Widmalm, G.; Mallnlak, A. *J. Phys. Chem. B* **2000**, 104, 6065.
  12. Jimenez, B. J. L.; Van Rooijen, J. J.; Erbel, P. J.; Leeftang, B. R.; Kamerling, J. P.; Vliegthart, J. F. *J. Biomol. NMR* **2000**, 16, 59.
  13. Imberty, A. *Curr. Opin. Struct. Biol.* **1997**, 7, 617.
  14. French, A. D.; Dowd, M. K.; Reilly, P. J. *J. Mol. Struct.* **1997**, 395, 271.
  15. French, A. D.; Brady, J. W. *Computer modeling of Carbohydrate Molecules*; American Chemical Society: Washington, DC, 1990.
  16. Christofides, J. C.; Davies, D. B.; Martin, J. A.; Rathbone, E. B. *J. Am. Chem. Soc.* **1986**, 108, 5738.
  17. Reynhardt, E. C.; Reuben, J. *J. Am. Chem. Soc.* **1987**, 109, 316.
  18. Adams, B.; Lerner, L. *J. Am. Chem. Soc.* **1992**, 114, 4827.
  19. Weimer, T.; Bukowski, R.; Young, N. M. *J. Biol. Chem.* **2000**, 275, 37006.
  20. Bekiroglu, S.; Sandstrom, C.; Norberg, T.; Kenne, L. *Carbohydrate Research* **2000**, 328, 409.
  21. Podolsky, D. K. *J. Biol. Chem.* **1985**, 260, 8262.
  22. Bekiroglu, S.; Sandstrom, C.; Norberg, T.; Kenne, L. *Carbohydrate Research* **2000**, 328, 409.
  23. Molecular Simulation Inc., San Diego, CA.
  24. Bodenhausen, G.; Freeman, R.; Niedermeyer, R.; Turner, D. L. *J. Magn. Reson.* **1977**, 26, 133.
  25. Bax, A.; Davis, D. G. *J. Magn. Reson.* **1985**, 65, 355.
  26. Kessler, H.; Gehrke, M.; Griesinger, C. *Angew. Chem.* **1988**, 100, 507.
  27. Bax, A.; Ikura, M.; Kay, L. E.; Torchia, D. A.; Tschudin, R. *J. Magn. Reson.* **1990**, 86, 304.
  28. Macura, S.; Ernst, R. R. *Mol. Phys.* **1980**, 41, 95.
  29. Bothner-By, A. A.; Stephens, R. L.; Lee, J. *J. Am. Chem. Soc.* **1984**, 106, 811.
  30. Brooks, S. R.; Bruccoleir, R. E.; Olafson, B. D.; States, D. J.; Swaminathan, S.; Karplus, M. *J. Comput. Chem.* **1983**, 4, 187.
  31. Liu, H.; Muller, F.; Gunsteren, W. F. *J. Am. Chem. Soc.* **1995**, 117, 4363.
  32. Burgi, R.; Daura, X.; Mark, A.; Bellanda, M.; Mammi, S.; Peggion, E.; Van Gunsteren, W. *J. Pept. Res.* **2001**, 57, 107.
  33. Kurnikova, M. G.; Balabai, N.; Waldeck, D. H.; Coalson, R. D. *J. Am. Chem. Soc.* **1998**, 120, 6121.
  34. Kessler, H.; Matter, H.; Gemmecker, G.; Di, H. J.; Isernia, C.; Mronga, S. *Intern. J. Pept. Prot. Res.* **1994**, 43, 47.
-